LCA Discussions

Efficient Information Visualization in LCA: Application and Practice

Harald E. Otto*, Karl G. Mueller and Fumihiko Kimura

Department of Precision Engineering, The University of Tokyo, Bunkyo-ku, Hongo 7-3-1, Tokyo 113-8656, Japan

* Corresponding author (otto@cim.pe.u-tokyo.ac.jp)

Otto HE, Mueller KG and Kimura F (2003): Efficient Information Visualization in LCA: **Introduction and Overview**. Int J LCA 8 (4) 183–189
Otto HE, Mueller KG and Kimura F (2003): Efficient Information Visualization in LCA: **Approach and Examples**. Int J LCA 8 (5) 259–265
Otto HE, Mueller KG and Kimura F (2004): Efficient Information Visualization in LCA: **Application and Practice**. Int J LCA 9 (1) 2–12

DOI: http://dx.doi.org/10.1065/lca2003.10.140

Abstract

Aim, Scope and Background. Acquisition and analysis of huge amounts of data still pose a challenge, with few options available for solutions and support. Life cycle assessment (LCA) experts face such problems on a daily basis. However, data do not become useful until some of the information they carry is extracted, and most important, represented in a way humans can both recognize efficiently and understand and interpret as quickly as possible. Unfortunately, information representation techniques as used in this field are still based on traditional low-dimensional information spaces, featuring only a few basic choices to represent life cycle (LC) related data. We must part from those traditional techniques and shift to visual representations that are easier for us to understand due to the human capability for detecting spatial structures and shapes represented in different colors and textures. Then all the advantages of modern, advanced information visualization can be applied and exploited.

Main Features. With the introduction of a new glyph-based information representation and visualization approach to LCA, current issues of representing LC-related information efficiently at a glance are being tackled. These new techniques support reduction of information load by providing tools to select and summarize data, assist in making explicit and transparent data feature propagation, and provide a means of representing data errors and uncertainty. In this approach the human perceptual capability for easily and quickly recognizing and understanding graphical objects in different colors and textures is exploited for the design and application of highly structured and advanced forms of multi-dimensional information representation.

Results. Now in the example presented in this paper, OM-glyphs were used to represent LCA-related information for an industrial product and its compiled life cycle inventory under conditions normal for LCA. To demonstrate the application and benefits of the approach introduced, several different visualization scenarios were computed and presented. These were illustrated with a selection of generated glyph-based displays containing spherical glyph clusters for environmental items such as air pollutants and water pollutants, and inventory glyph matrices related to components and to LC phases. Where appropriate, to further aid understanding and clarity, displays were additionally shown with various orientations and in enlarged form. This is a functional feature of interactive 3D OM-glyph based information visualization that can be used in practice to efficiently navigate through displays while at the same time adjusting rendered scenes to the needs of the user at any given time. Due to the huge amount of data acquired and compiled, only a small fraction of the glyph-based displays could be shown, and, in consequence, only a fraction of the data properties, patterns and features available could be discussed in detail. However, it is believed that the basic principles and methods of this approach, as shown in a real application, could be clearly conveyed, and, most important, that the benefits and potential could be displayed in a convincing manner. This technology will support a marked increase in efficiency, speed and quality in LC information analysis.

Conclusions. This paper concludes our short series on efficient information visualization in LCA. A new approach to efficient information visualization has been introduced, together with its basic principles. This background was enriched with discussions on and further insights into technical details of the approach and the framework developed. The first practical examples were provided in the previous paper, demonstrating the mapping of LCA-related data and their contexts to glyph parameters. In this paper the application of the approach was presented using data for an actual industrial product. During the discussions, and with the various glyph-based displays shown, it could be convincingly demonstrated that all data features, trends, patterns, relationships, and data imperfections detected and examined, and sometimes traced, could be quickly and efficiently recognized in a short time. Even basic data features, such as small gaps in the data propagation of related values, could be easily seen using OM-glyphs. In the case of traditional data representation, using for example LCI tables, this would require the identification and comparison of several thousand numerical entries. As is the case with all new technology, however, it is still difficult to obtain the interest of the experts, and to convince them that such new ideas will eventually change the face of industry.

Outlook. A new, advanced and efficient information representation and visualization approach has been introduced to the LCA community. Hopefully, through this small series of papers, some interest will have been generated in the field of advanced information visualization. For the first time this area has been related to LCA, and some seeds for interdisciplinary research may have been sown. Now it is up to individuals, the experts in the various fields related to those issues, to respond. The desired results will be stimulating discussions, an exchange of ideas, further initiated multilateral, interdisciplinary efforts, and improved collaboration between partners from academia and industry. At that point, efficient information visualization will finally have arrived at, and received, its deserved place within LCA.

Keywords: Glyph rendering; information visualization; life cycle assessment (LCA); life cycle data set mapping; life cycle inventory (LCI); multi-dimensional information space

1 Goal and Scope

Computer-aided support is still in its infancy for the acquisition and analysis of the typically huge amounts of data which a life cycle assessment (LCA) expert may face every time a product and its life cycle (LC) are systematically examined. The methods, technologies and tools provided are inadequate, old-fashioned, and in most cases of a low degree of inter-operability and integration. Innovation of methods, technologies and tools is essential to support successful translation of assessment frameworks (ISO14040) into practice. This is especially true for information representation in data-intensive fields such as LCA. Unfortunately, compared with other engineering-related fields, not much has been achieved yet. At this point, it should be emphasized again that data do not become useful until some of the information they carry is extracted, and, most important, represented in a way humans can both recognize efficiently and understand and interpret as quickly as possible. We must move from traditional data representation techniques such as 2D and 3D variants of simple tables, bar charts, x/y graphs, etc., and shift to visual representations that are easier for humans to understand due to their perceptual capabilities for detecting spatial structures and shapes represented in different colors and textures. Thus, all the advantages of modern, advanced information visualization can be applied and exploited. For these reasons, a pictorial representation based on OM-glyphs, a special class of interactive, three-dimensional geometric object, has been developed and introduced. This novel approach represents an alternative, though advanced and highly flexible, means to efficiently represent and visualize information in LCA. In particular, this approach supports reduction of information load by providing tools to select and summarize data, offering to make explicit and transparent data feature propagation, and providing a means of representing data errors and uncertainty.

Within this short series on efficient information visualization in LCA, which will come to a temporary conclusion with this paper, the following issues have been targeted and presented. In the first paper, the motivation for this novel approach was introduced and the basic concept and some fundamental principles of glyph-based visualization techniques were discussed. In the second paper, more technical details of the approach and the framework implemented were introduced. Also, issues concerning individual visualization scenarios and the mapping of LCA related data and contexts were presented and discussed. Additional examples were provided of techniques used for the visualization of data uncertainty and of filtered absolute and relative contributions to quantities of energy requirements and environmental items, both as related to individual life cycle phases, and as products or their parts and components. Now, in this last paper of the series, further details regarding two advanced visualization structures, namely glyph matrices and spherical glyph clusters, will be presented. Information will be provided on the spatial arrangement of glyphs within those structures and an outline will be given of the mapping to entities of another related data structure, a product tree. Aspects of application and translation into practice will be presented, together with examples using real industrial product data.

2 Background and Problems

A brief review on background and problems is given in the following. This will assist recall and highlight once again the basics of information visualization as far as they relate to the problems of efficient representation and visualization of information regarding an application field as addressed within the approach introduced. This review should be sufficient to summarize the major and most important issues, and the problems addressed and discussed. However, it is kept brief, as are the selected references to related work, due to the numerous details and references already given in the previous papers of this series.

Information visualization is concerned with the efficient transformation and mapping of data and context to a visual representation easy for humans to understand. The concept of exchanging data and context for a well-structured representation using geometric objects was investigated in early work on the theory and principles of pictorial representations (Feibleman 1969, Bertin 1983, Chang 1989) and also within logics and semiotics. Results of successful developments and applications of such advanced geometric objects, called icons and glyphs, are documented in (Ribarsky et al. 1994, Post et al. 1995, Abello et al. 2000). Appropriate and natural as the basic principles of information visualization appear, taking into account the fact that visual representations are easy for humans to understand, there are still problems with relating data and context efficiently to a meaningful visual representation (cf. Cleveland and McGill 1995, Card and Mackinlay 1997, Yang-Paláez and Flowers 2000, Nowell et al. 2002). These problems have not yet been solved completely. See also the review and discussion of perceptual issues pertaining to information visualization presented in (Ware 2000). Also the design of three-dimensional shapes for graphical objects in different colors and textures, easy for humans to recognize and understand, while at the same time featuring a highly structured and advanced form of information representation (Parker et al. 1992, Ebert et al. 2000), is still a problem that must be solved individually within each particular application field. However, once such initial hurdles have been overcome for a particular application field, advanced information visualization permits the development and use of (computer-aided) tools. These elevate data-intensive and human-depended tasks, such as multi-dimensional simultaneous representation of huge amounts of data, recognition of data features and their propagation, and advanced information interpretation and analysis, to levels of complexity, performance and efficiency, which are far beyond the capabilities of traditional data representation methods.

3 Advanced Visualization Structures

3.1 Overview

In principle, OM-glyphs as introduced can be used to visualize any LCA-related information within any visualization scenario, as shown and discussed earlier in this series. However, it is desirable to visualize efficiently as many dimensions and viewpoints as possible of such information within a multi-dimensional information visualization space, while

also representing additional structural data properties such as product internal relationships linked to entities of the LCI data space, data feature propagation, etc. Visualization structures more advanced than OM-glyphs are required for this.

In the following two sections, further technical details of two advanced visualization structures, namely glyph matrices and spherical glyph clusters, will be presented. Within previous papers in this series on information visualization in LCA, the basic elements of those advanced visualization structures, OM-glyphs, have been introduced and discussed in detail. Therefore details of OM-glyphs will not be repeated, though, where necessary, references to previously published material are given. Technical details on glyph matrices and spherical glyph clusters presented in the following include an insight into the spatial arrangements of OM-glyphs within those advanced visualization structures, information on their data structure and an outline of the mapping to entities of yet another related data structure, a product tree.

3.2 Glyph matrices

In mathematics and other related fields, rectangular arrays of numbers are called *matrices*. Due to similarities with these numerical matrices in both the spatial arrangement of entries and some properties of the data structure itself, glyph formations as already introduced in the previous two papers of this series on information visualization, and also as shown in Figure 4, are called *glyph matrices* ($GM^{(m,n)}$). In mathematics, the entries in matrices may be either real numbers or complex numbers represented by an efficient notation as used in the literature and also shown in the appendix. Glyph matrices have as entries rendered, fully interactive OM-glyphs with a spatial arrangement that will be described below in detail. Glyph matrices consist of rows and columns, indicating not their dimension related to an abstracted entity space as in the case of row vectors and column vectors within a matrix in mathematics, but their size and spatial arrangement related to a grid. Within a glyph matrix each glyph is positioned with its glyph origin at one intersection point of this grid.

To avoid spatial interference of rendered glyphs within a glyph matrix, computation of the distance between each intersection point of the grid in the y-direction (width w_g) and z-direction (height h_g) needs to take into account the size of the largest glyph within a glyph matrix and a correction factor related to the size and geometry of the pixels of the computer screen. Using the size of the half-axis a_{max} of the central sphere of the largest glyph, a factor k can be defined so that it relates within a glyph the maximum dimensions of the central sphere and ellipsoids attached, and horizontal and vertical correction factors c_h and c_v. Distances in each direction between each intersection point of the grid can be defined as shown in Eq.1 and Eq.2.

$$w_g = 2\,((k+1)\,a_{max}\,c_h) \tag{1}$$

$$h_g = 2\,((k+1)\,a_{max}\,c_v) \tag{2}$$

To assign a glyph's geometrical components to their proper location within a glyph matrix while also adjusting the orientation of the glyph so as to visualize a maximum of information at a glance, a set of matrices defining translation and rotation (see appendix) is required. Basically this set of matrices, denoted as type $\boldsymbol{L}$, includes a translation matrix to move the glyph to the origin of the coordinate axes (in case it is located otherwise), individual rotation matrices for each axis, and a translation matrix to position the glyph in its final location within the grid of the glyph matrix. The computation of such a location matrix for one instance $L \in \boldsymbol{L}$ in the form of a matrix product is shown in Eq.3.

$$L = T_{xyz}\,(R_x\,R_y\,R_z)\,T_{xyz} \tag{3}$$

The last component that is required to complete the description of the glyph matrix structure is a scaling factor in form of a scaling matrix $S_{xyz} \in \boldsymbol{S}$ (see Eq.8 in the appendix) to define adjustments in the size of the glyph. Annotation $\boldsymbol{A}$, if switched on, is a cross product of information regarding color, size, font, location (lower left corner of the bounding box of the first character), and string sequence required to create a piece of text attached to a glyph. Now the complete structure of an $m \times n$ glyph matrix $GM^{(m,n)}$ can be formally described using the type G for glyphs introduced earlier in (Otto et al. 2003b), as shown in Eq.4.

$$\begin{aligned} GM^{(m,n)} &= (G_{11} \times \boldsymbol{S} \times \boldsymbol{L} \times \boldsymbol{A}) \times \ldots \\ &\times (G_{m1} \times \boldsymbol{S} \times \boldsymbol{L} \times \boldsymbol{A}) \times \ldots \\ &\times (G_{mn} \times \boldsymbol{S} \times \boldsymbol{L} \times \boldsymbol{A}) \end{aligned} \tag{4}$$

A single glyph in a glyph matrix is denoted as $g(i,j)$, representing the glyph located at the intersection point of the i-th row and the j-th column of the grid. Note that the indices on the glyph types used are introduced only to increase the readability of the equation. Some denotations of types introduced here are in boldface to help distinguish more easily a type from an entity such as a matrix which is denoted using italic capitals.

3.3 Spherical glyph clusters

Yet another advanced visualization structure, though more complex and powerful than glyph matrices, is *spherical glyph clusters* ($SGC^{(m,n)}$). A first example was informally introduced in (Otto et al. 2003b), and further examples will be shown and discussed in a later section of this paper. Spherical glyph clusters were developed to represent within a multi-dimensional information visualization space LCA-related information that can be linked to a product tree (for more details about tree-based data structures see appendix). Their principal purpose is to combine LCA-related information with structural properties and relationships intrinsic of a product and its components. Within a product tree the root represents the entire product, while sub-trees with their roots and nodes represent individual components and their related assemblies and sub-assemblies of parts. Those parent / child relationships of the entire product tree are preserved fully

within a spherical glyph cluster. In particular the following structural features between a product tree and a spherical glyph cluster are mapped. The root of the product tree is related to the glyph located at the origin of the spherical glyph cluster, which is called the *spherical glyph cluster center*. Each node of the product tree that can be also a root or a leaf of a sub-tree is related to a glyph within a spherical glyph cluster, and this glyph is termed a *regular glyph*. In particular, each root of a sub-tree at height or level n is related to a glyph at cluster level n (see nested spherical hulls below) within a spherical glyph cluster, which is called *inner glyph*. Each node that represents a leaf is related to a glyph, and this glyph is an *outer glyph*. In particular, glyphs that are related to the leafs of the entire product tree are called *satellite glyphs*, since they are located at greatest distance (inner path) from the spherical glyph cluster center. The weight, i.e. number of glyphs in a spherical glyph cluster, is less than or equal to the weight of the product tree. The level, i.e. number of spherical hulls (see discussion below), of a spherical glyph cluster is less than or equal to the height or levels of a product tree. Also the inner path length and average path length of a spherical glyph cluster are less than or equal to their counterparts in the product tree.

The spatial arrangement of glyphs within a spherical glyph cluster is based on nested spherical hulls denoted as H. Each spherical hull represents a convex spherical reference surface for spatially locating glyphs that are related to product tree nodes. Each ascending tree level is related to one of the hulls extending concentrically from the glyph cluster origin and enclosing all previous smaller hulls being related to lower tree levels. To avoid spatial interference of glyphs located on the surface of such spherical hulls, while providing equidistant spacing between the hulls, the following parameters need to be taken into account in computing the dimensions. The mean $\overline{cn_i}$ of the related LCI contribution cn_i in cases where data uncertainty is modeled by providing lower limit and upper limit values. The level number n, corresponding to the level of the related product tree. The sphere / ellipsoid dimension factor k (see again Eq.1 and Eq.2) and the mapping factor b taking into consideration the method of relating LCI contributions to the dimensions (b = 1), the surface (b = 1/2), or the volume (b = 1/3) of a glyph (see again Otto et al. 2003a, p. 186–187). Computation of the half-axis $a^{(n)}$ of a spherical hull at level n can be described now as shown in Eq.5.

$$a^{(n)} = (k+1)\,(|\,\overline{cn_i}\,|)^b\,(n+1) \tag{5}$$

The exact location of an individual glyph on the surface of a spherical hull is computed by determining the coordinates of points p_n on the surface, based on the angle of elevation of a vector $\overrightarrow{Op_n}$ (between the origin O and p_n) and a plane located at the origin of the spherical hull with its normal $\boldsymbol{n} \in \mathbf{R}^3$ being collinear to the z-axis. Assignment and sectioning of circles with those angles of elevation computed on a spherical surface are determined employing sub-division based on prime factorization and taking into account the number of glyphs related to a spherical hull at cluster level n within the spherical glyph cluster (Otto and Mueller 2002a). Final results in the form of entries for translation matrices and rotation matrices, combined into one location matrix, can be obtained and used later for computation, as already shown in Eq.3. Each regular glyph within a spherical glyph cluster contains also an edge with a type denoted as D that visualizes the link between this (child) glyph and its (parent) glyph. This edge is rendered in the same color as the central sphere of the glyph. The edge is represented as a straight line connecting the centers with coordinates p_m and p_n of both glyphs, the parent glyph and the child glyph. Using a scalar $\lambda \in \mathbf{R}$, the edge can be described in vector notation as shown in Eq.6.

$$\boldsymbol{x} = p_m + \lambda \overrightarrow{p_m p_n} \tag{6}$$

Finally, by including also a scaling factor in the form of a scaling matrix (see again previous section on glyph matrices), the structure of a spherical glyph cluster $SGC^{(m,n)}$ of weight m with n cluster levels can be described as shown in Eq.7.

$$\begin{aligned} SGC^{(m,n)} &= (G_0 \times \boldsymbol{S} \times \boldsymbol{L}) \times (G_1 \times \boldsymbol{S} \times \boldsymbol{L} \times D) \times \ldots \\ &\times (G_{m-1} \times \boldsymbol{S} \times \boldsymbol{L} \times D) \times H_1 \times \ldots \times H_{n-1} \end{aligned} \tag{7}$$

A single glyph of a spherical glyph cluster is denoted as $g(i,j)$, representing the i-th glyph located on the (reference) surface of the j-th spherical hull. Note that the glyph in the center of the spherical glyph cluster does not have an edge associated with it, because it has no parent glyph to which it is related (cf. first term in Eq.7). Again the indices on the glyph types and the spherical hull types used are introduced only to increase the readability of the equation. More technical details of the data structure and its notation can be found in (Otto 2003).

4 Information Visualization in Practice

4.1 Outline

As mentioned previously, in this final section the application of glyph-based information visualization will be presented using the full data set for a real industrial product. Data used to compile the LCI in the application example were taken from an integrated product data base courtesy of a large Japanese manufacturer of electronic appliances and computers. The product examined was a desktop computer complete with color monitor, keyboard, mouse, etc. and consisted of a total of 135 components and parts. For the information visualization demonstration and the discussions, compiled data sets of two selected examples were presented. These were the contribution of the air pollutant fossil carbon dioxide (CO_2) in relation to product components and to life cycle phases and the contribution of the water pollutant lead in relation to product components and to life cycle phases. Computations were carried out for a product life cycle consisting of seven basic phases (see details below). Due to the great amount of numerical data compiled for the examples, consisting of over 2800 entries for one environmental item, basic LCI tables have been omitted. However, where appropriate, to aid understanding and clarity, concrete numerical values will be given together with rendered glyph-based data displays.

4.2 Basic values and settings

For the visualization, basic settings and assignments are as follows. Absolute values of contributors are proportional to the volume of each sphere. Relative values of contributors are proportional to the volume of related ellipsoids attached to each sphere (see Otto et al. 2003a, p. 186–187). Individual life cycle phases considered are encoded and assigned colors as follows: pre-manufacturing (PM, black), manufacturing (M, red), use (U, green), post-use with recycling (PURC, yellow), post-use with re-manufacturing (PURM, violet), post-use with re-use (PURU, magenta), and post-use with disposal (PUD, cyan). The glyph filter is generally set at zero in the visualization displays shown. If it is set at another value, that is explicitly indicated, and the filter value given.

The product tree consists of one root, representing the desktop computer unit and the color monitor together, and three further levels of sub-trees, representing each of the 135 components and parts with their nodes and leafs, as shown in Fig. 13. The mass of the desktop computer and the color monitor were 10 kg and 12 kg, respectively. The electric power input required was 100 watts for each. The profile for the use phase in the example was set to eight hours per day for 200 days per year over a period of two years.

4.3 Analysis and interpretation of visualized data

To obtain an overview and a first estimate of how absolute and relative contributions of CO_2 are related to components and parts in regard to each life cycle phase, it is best to examine a spherical glyph cluster for carbon dioxide emissions as shown in **Fig. 1**.

In this glyph-based display, the components and parts, representing the main contributors of CO_2, are visible at a glance. They are represented by the largest glyphs in the display, surrounding the spherical glyph cluster center at different cluster levels. For the example shown, these are on the second cluster level and are the desktop computer unit, with a total CO_2 contribution of 190.6 kg, represented by the glyph *g(1,1)* with a large light gray sphere in the center, and the color monitor, with a total CO_2 contribution of 188.3 kg, represented by the glyph *g(2,1)* with a large light red sphere in the center. As can be seen from the display and the glyph identifiers, both glyphs are located on the surface of the first spherical hull (see again second glyph index and Eq.7). Since they are inner glyphs, they correspond to the roots of the two sub-trees located directly beneath the root of the product tree (cf. node 2 and node 3 in Fig. 13).

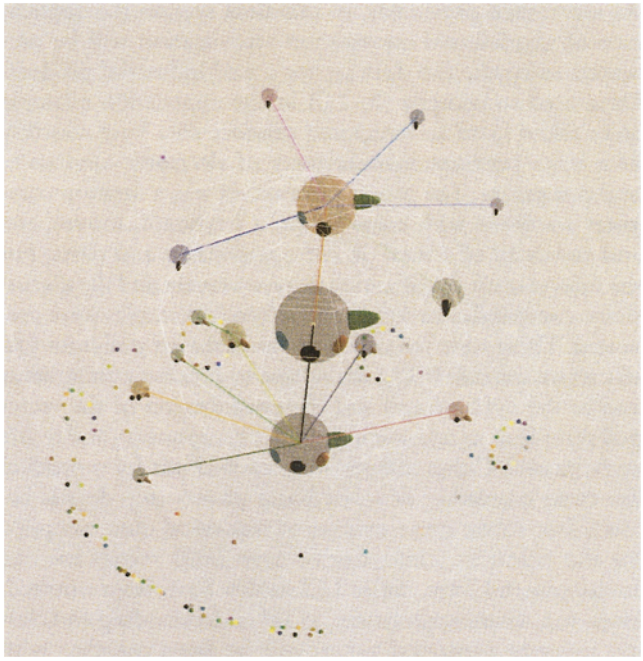

Fig. 1: Spherical glyph cluster for carbon dioxide emissions

The glyphs connected with *g(1,1)* and *g(2,1)* and located on the surface of the second spherical hull will be examined in detail next. In the case of the desktop computer unit, several large outer glyphs can be recognized at a glance. These represent the main sub-contributors: the keyboard (ochre yellow sphere), the motherboard (light green sphere), the electric power supply (light violet sphere), and the CD-RW unit (light red sphere).

Similar examinations regarding the emission of CO_2 in respect of other components and parts can be carried out for all (relevant) contributors. One first locates their representative glyph in the display and then evaluates and compares their spheres and spheroids. Small contributions are represented by tiny glyphs located on the surface of the same spherical hull and appear in the display as small dots among the larger glyphs. In this visualization scenario, the contributions of individual parts, represented as leafs within the product tree, are very small and therefore appear in Fig. 1 and **Fig. 2** only as tiny (satellite) glyphs located on the surface of the third spherical hull.

To examine now which LC phase is dominant regarding the CO_2 emissions of large contributors, the ellipsoids of previously examined glyphs can be used. For the entire product, the ellipsoids of the glyph cluster center, represented by glyph *g(1,0)*, indicate that the use phase (green ellipsoid) is dominant, representing a relative contribution of 285.14 kg, i.e. 75.3%. The second and third most dominant LC phases in relation to the emission of CO_2 are pre-manufacturing (black ellipsoid) with 63.3 kg, i.e. 16.7%, and manufacturing (red

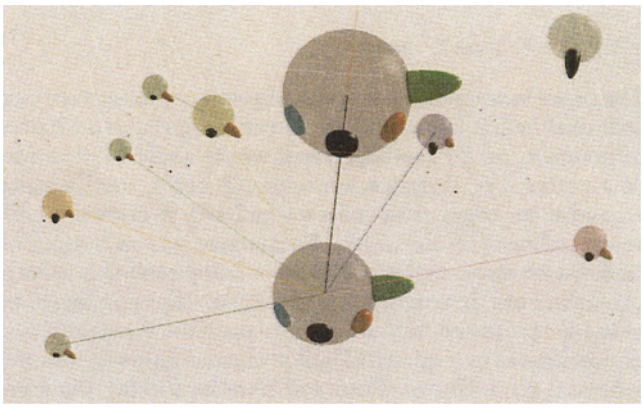

Fig. 2: Enlarged section of a spherical glyph cluster for carbon dioxide emissions

ellipsoid) with 29.1 kg, i.e. 7.6%. Emissions of CO_2 are lowest in the post-use with disposal phase (cyan ellipsoid) with 1.4 kg, i.e. 0.4%.

All OM-glyph based visualizations consist of interactive 3D objects that can be manipulated by the user, to adjust among other properties, orientation and size. An enlarged view of the lower part of the spherical glyph cluster in Fig. 1, featuring the spherical glyph cluster center and a large inner glyph with several connected smaller outer glyphs, is shown in Fig. 2. Now, in this enlarged display, the dominance of LC phases regarding the emission of CO_2 can be seen at a glance, and is as clear as it was in the case of the spherical glyph cluster center. For example, in the case of the motherboard (fourth glyph on the left with light green sphere), manufacturing (red ellipsoid) with 10.5 kg is more dominant than pre-manufacturing (black ellipsoid) with only 2.6 kg of CO_2 emissions. In the case of the electric power supply (second glyph on the right with light violet sphere) the situation is just the opposite, with pre-manufacturing more dominant than manufacturing. Again, a similar examination revealing the dominance of LC phases regarding CO_2 emissions can be carried out for each component and part by first visually locating the representative glyph and then evaluating its ellipsoids. Perhaps, for this purpose, it is better to change the view of the display several times during the examination. A snapshot of the display showing the spherical glyph cluster of Fig. 1 turned around the y-axis is given in **Fig. 3**.

In this realigned display, the comparative ellipsoid sizes of the dominating use phase, in green, and of the manufacturing phase, in red, can be seen most clearly.

Besides the value propagation and dominance of entities, another feature can be easily recognized. This is the absence of values, i.e. gaps in a traced sequence of related values. For example, for the monitor no CO_2 emission values were available for the manufacturing phase. This can be easily and quickly recognized if examine again the glyph *g(2,1)* in Fig. 1. The red ellipsoid that can be traced in other connected glyphs is missing. To find such a data gap manually, and relate it to a particular component and LC phase within a set of traditional LCI tables, would require the examination of thousands of numerical entries.

Another data feature that can be quickly recognized and efficiently traced is data imperfection caused by uncertainty and errors. In the spherical glyph cluster in Fig. 1, one glyph featuring at its center a spheroid instead of a sphere can be recognized immediately at the right. It is one of the outer glyphs of glyph *g(2,1)* with a light emerald green spheroid at its center. It represents the cathode ray tube (CRT) assembly and is connected by its edge to the glyph representing the monitor as contributor. It is spatially positioned on the surface of the second spherical hull (see also upper right in Fig. 2). Its shape distortion reveals that the average CO_2 emission for the CRT assembly is much closer to an upper limit than a lower limit (Otto and Mueller 2002, Otto et al. 2003b). To further trace this detected data imperfection and determine from where it may stem, a brief look at the base inventory glyph matrix can be of assistance.

In **Fig. 4**, the base inventory is visualized as a glyph matrix $GM^{(5,6)}$ with 27 normalized and standardized glyph spheres. In this display, items with absolute contributions in different units cannot and must not be compared with each other on a quantitative base using a glyph sphere. Data imperfections represented as spheroids within glyphs can be quickly recognized for glyph *g(1,5)* representing copper, glyph *g(2,5)* representing glass, glyph *g(4,6)* representing generic rubber, and glyph *g(5,3)* representing stainless steel, all major materials in a CRT assembly. To double-check the assumption of traced data imperfection, another base inventory glyph matrix, related to components and parts, can be consulted. Note that since examples of complete inventory glyph matrices have been already given, in the following only glyph submatrices containing glyphs relevant to the discussion will be presented. This enables greater detail to be shown, since a display containing a small number of glyphs can be shown in a larger format.

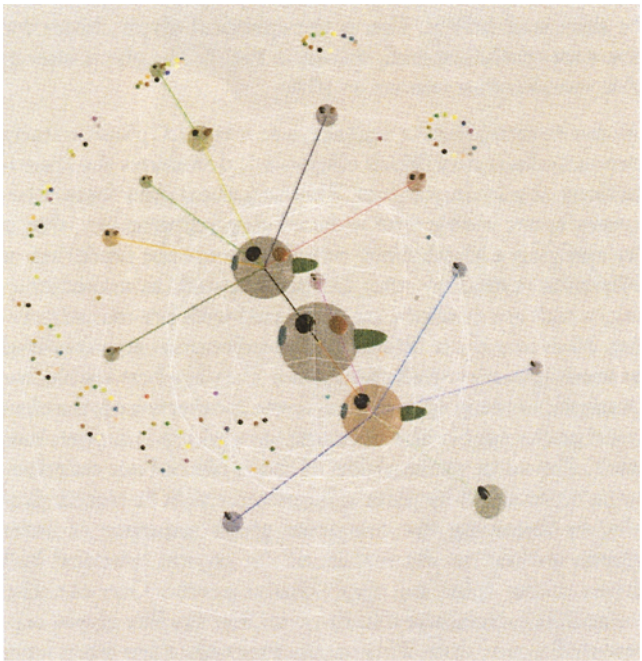

Fig. 3: Spherical glyph cluster for carbon dioxide emissions with varied orientation

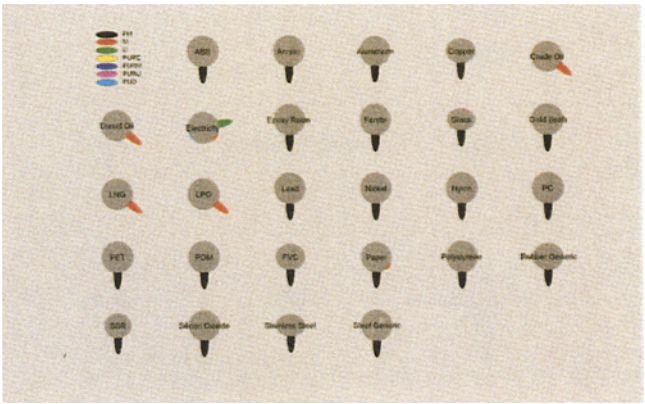

Fig. 4: Glyph matrix as related to inventory items and life cycle phases

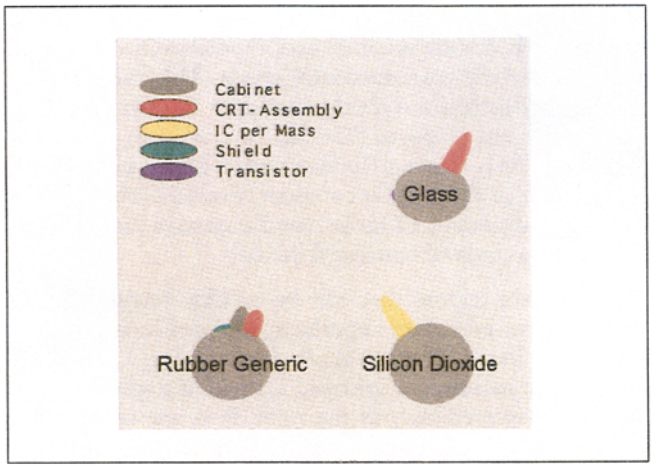

Fig. 5: Glyph sub-matrix as related to inventory items and to components and parts

For example, in the case of generic rubber, represented by glyph *g(2,1)* in the glyph sub-matrix depicted in **Fig. 5**, one relative contribution amounts to 48.2%, i.e. 0.3 kg, in the CRT assembly (red ellipsoid). In the case of glass, represented by glyph *g(1,2)*, one relative contribution amounts to a very dominant 99.5%, i.e. 5.5 kg, in the CRT assembly, while the other relative contribution for the transistors (tiny dark blue ellipsoid on the left) remains insignificant at only 0.5%, i.e. 27.6 gr. Note that in the case of silicon dioxide represented by glyph *g(2,2)*, an example is given, to demonstrate a relative contribution (IC per mass, ochre ellipsoid), which at an amount of 32.5 gr. is equal to the absolute contribution of the item represented. Another way to examine and verify the detected data imperfection in the CRT assembly is to analyze the display of the component matrix as related to the item (CO_2 emissions) traced and to LC phases.

In **Fig. 6**, a glyph sub-matrix $GM^{(3,3)}$ has been extracted from the much larger CO_2 glyph matrix. In this display, the glyph

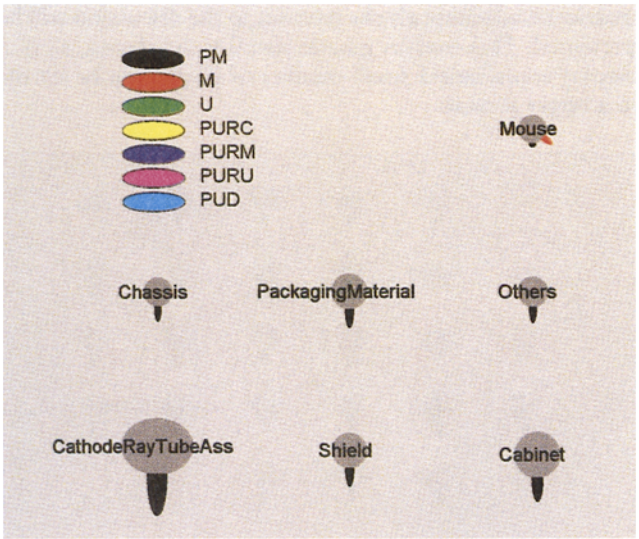

Fig. 6: Carbon dioxide glyph sub-matrix as related to components and to LC phases

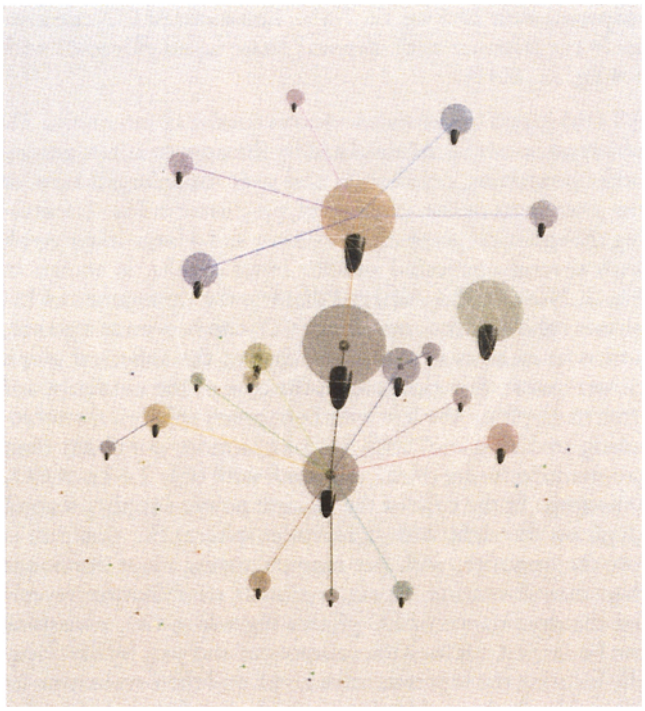

Fig. 7: Spherical glyph cluster for lead emissions

g(3,1) related to the CRT assembly represents very dominant CO_2 emissions for the pre-manufacturing phase with the same type and structure of data imperfection as previously seen in the spherical glyph cluster in Fig. 1 and Fig. 2.

The example given was for only a single environmental item, the air pollutant carbon dioxide. The same type of display can be generated for any inventory item or environmental item. An example for demonstration purposes only will now be discussed briefly. This is the spherical glyph cluster for the water pollutant lead, shown in **Fig. 7**. The glyph filter in this visualization was set at 10%.

As can be recognized at a glance, one major LC phase, namely pre-manufacturing (black ellipsoids), dominates the contributions of all components. This structural data feature becomes better visible with reduced glyph dimensions, that is by applying a glyph filter, which prevents the rendering of ellipsoids related to other LC phases, such as manufacturing, which are insignificant compared with pre-manufacturing. Note that these filtered out contributions are visualized as inner spheres within the glyphs. They are best visible, for example, in the glyphs related to the motherboard, the electrical power supply and of course the desktop computer unit itself. The value propagation of those filtered out contributions represented by inner spheres can easily be traced visually, by following the connected glyph sequence of outer glyphs located on the surface of the second spherical hull down to the spherical glyph cluster center. One can also immediately recognize that there are few satellite glyphs represented as tiny dots. This means that only a few parts have absolute contributions that are large enough to be rendered as visible entities in the display. Also, the data imperfection

within the outer glyph related to the CRT assembly (light emerald green glyph on the right with a spheroid at its center) can be recognized at a glance, though its dimensions, thus its dominance and impact, are different from those in the previous example for carbon dioxide.

Note that absolute contributions as shown in Fig. 7 are very small, remaining in the range of only a very few milligrams or even micrograms. Therefore, as mentioned earlier, glyphs in different displays related to different items cannot be used directly to compare absolute contributions by comparing the sizes of the spheres and spheroids. However, work is being undertaken to provide concrete data for interactive quantitative analysis on demand by employing explicit system feedback. It is planned to enhance OM-glyph based visualization structures with context-sensitive pull-down data menus associated with each glyph. When this system extension has been completed, a user will be able to select any component of any glyph by using a pointing device such as a mouse or a stylus. The user will then select from a pull-down menu, appearing within a small window, concrete data such as the exact name of the item represented, inventory type and identifier, contribution type/unit and value, or exact location.

Many more data features and relationships can be found in the glyph-based displays shown. However, these will not be discussed in detail, since this aim of this paper was not to present yet another example of complete life cycle analysis of an industrial product, but to demonstrate the application and benefit of the approach introduced and presented within this series of papers. The testbed currently implemented provides for the computation of over a hundred major energy, material and environmental items. Examination strategies and generated displays as presented can then be used to support comparison and analysis of structural properties and data features of those various items.

As demonstrated in this example, the basic features of a large LC-related data set such as absolute and relative contributions, item distribution, dominance of contributing components and parts, importance of LC phases, or data imperfection can be seen very rapidly in a glyph-based display. Such a display supports a type of 'visual arithmetic', as one looks at the various glyphs and compares their geometrical, spatial and retinal properties. Using the example presented and discussed, traditional data representation would require that an expert look simultaneously at several tables representing various values for entries, expressed sometimes in physical units and sometimes in percentages. These would consist of the calculated carbon dioxide emissions of 135 components and parts across several life cycle phases. A heavy mental load and considerable challenge would be imposed upon the human visual system of the expert. One would need to examine and recognize the significance of thousands of numerical values, then assess them in relation to each other and make necessary comparisons. Only at that point could an expert start to make the most obvious of the statements which are clearly visible using OM-glyph based visualization.

5 Conclusions

Within this paper, details of advanced visualization structures were presented using again a mostly informal style, to keep explanations transparent. In particular, issues concerning the spatial arrangement of glyphs within glyph matrices and spherical glyph clusters, and entity mapping between spherical glyph clusters and product trees were addressed. A selection of meaningful results was presented from a full application of the approach and the framework developed. These results demonstrated application and performance under conditions customary in practice using actual product data and LC data of a real industrial product. In particular attention was given to issues of user-based display control, multi-dimensional information representation, recognition and interpretation regarding amount of information in a rendered display / scene, absolute and relative contributions, data uncertainty and errors, entity relationships and patterns, anomalies, trends, and data feature propagation.

Information visualization transforms (mostly numeric) data into a visual form that provides an alternative for exploring various ways of looking at data. However, trying to understand the reality or to develop concepts by examining information in this way, depends on the quality of the data and the quality and effectiveness of the presentation method used. Within the approach and framework introduced and presented, those issues have been addressed as follows. Imperfection and uncertainty of data is represented by variations in the appearance of the object. Thus, the representation is intrinsic. Extrinsic representations, requiring additional objects such as question marks, arrows, etc., have been avoided, since they tend to lead to information overload. However, sound principles governing the understanding of imperfect information by using representations at this stage of development have not yet been perfected. Similarly, guidelines are also lacking on reaching sound conclusions and decisions in practice. Since too many details tend to overwhelm a user, and also contribute to information fatigue, additional information such as display date, scene title, etc. have been regarded as 'eye candy', and omitted. This avoids distracting the user's attention from important pieces of information. Also the object design and graphics layout as described do not contain any irrelevant elements. There are no aesthetic or decorative elements such as border lines or frames. Every element and every component is precisely defined regarding the mapping between its attributes and object semantics. Only objects which are really identical are represented with exactly similar values, thus appearing in the visualization space as identical entities. To avoid users being forced to exert their mental powers to interpret unsuitable designs, the structure and appearance of OM-glyphs were specifically formulated to meet requirements customary in LCA. During the design process the main focus was always on how to optimize representation in terms of supporting the recognition of data features, trends, anomalies, etc. In this way additional, valuable information will be revealed. The representation of LC-related data solely for the purpose of obtaining a record was not and was never intended be the main focus. Nevertheless it has to be recognized that one faces a considerable challenge in walking the line between the degree of abstraction regarding the data representation and the amount of information shown in the display.

As is the case with all new technology, it is difficult to obtain the interest of the experts, and to convince them that such new ideas will eventually change the face of industry. Information visualization is no exception in this respect. In the meantime we have to overcome two major barriers: natural human resistance to any form of change, and the lack of well-understood principles upon which scientific visualization can be based in order to become a sound and recognized discipline of its own.

6 Recommendation and Outlook

The work presented in this series, has specifically brought efficient glyph-based information representation and visualization to LCA and its community for the first time. Due to the interdisciplinary nature of the work, a carefully designed presentation has been provided, with references to supplementary literature, offering a transparent and easy to understand synopsis on background and basic principles and methods used. This presentation has been enriched with several short, easily comprehended examples aimed at demonstrating applications of the methods and structures employed. It has also offered a full application using industrial product data, to demonstrate the translation of the technology and its framework into practice. It is hoped that such an approach will be able to reach and stimulate a broad spectrum of experts from various related disciplines in both academia and industry.

References

Abello J, Korn J (2000): Visualizing massive multi-graphs. In: Proc. of the IEEE Symposium on Information Visualization'00, October 9–10, Salt Lake City, Utah, USA, 39–47

Aho AV, Ullman JD, Hopcroft JE (1983): Data Structures and Algorithms, Addison-Wesley, Reading, Massachusetts, USA

Berg M, Kreveld M, Overmars M, Schwarzkopf O (1997): Computational Geometry, Algorithms and Applications. Springer-Verlag, New York, USA

Bertin J (1967/83): Semiology of Graphics: Diagrams, Networks, Maps. The University of Wisconsin Press, Madison, Wisconsin, USA

Card SK, Mackinlay J (1997): The Structure of the Information Visualization Design Space. in: Proc. of the IEEE Symposium on Information Visualization'97, Phoenix, Arizona, USA, 92–99

Chang SK (1989): Principles of Pictorial Information Systems Design. Prentice-Hall, Englewood Cliffs, New Jersey, USA

Cleveland WS, McGill R (1995): Graphical Perception and Graphical Methods for Analyzing Scientific Data. Science, 229, 828–833

Ebert DS, Rohrer RM, Shaw CD, Panda P, Kukla JM, Roberts DA (2000): Procedural shape generation for multi-dimensional data visualization. Computers and Graphics 24, 375–384

Feibleman JK (1969): An Introduction to the Philosophy of Charles S. Pierce. MIT Press, Cambridge, Massachusetts, USA

Golub GH, van Loan CF (1996): Matrix Computations. The Johns Hopkins University Press, Baltimore, USA

Hosaka M (1992): Modeling of Curves and Surfaces in CAD / CAM. Springer-Verlag, New York, USA.

ISO 14040 ff. DIN EN ISO 14040 ff: (1997) Umweltmanagement – Ökobilanz. Beuth, Berlin, Germany

Maxwell EA (1951): General Homogeneous Coordinates in Space of Three Dimensions. Cambridge University Press, Cambridge, USA

Nowell L, Schulman R, Hix D (2002): Graphical Encoding for Information Visualization: An Empirical Study. In: Proc. of the IEEE Symposium on Information Visualization'02, October 28–29, Boston, Massachusetts, USA, 43–50

Otto HE, Mueller KG (2002a): Structure and Evolution of Advanced OM-Glyphs. Research Note CR-KLO-03-02, Department of Precision Engineering, CAD/CAM Research, University of Tokyo

Otto HE, Mueller KG (2002b): Computation of OM-Glyph Locations within Spherical Glyph Clusters. Research Note RN-KLO-06-02, Department of Precision Engineering, CAD/CAM Research, University of Tokyo, Japan

Otto HE (2003): On Notation and Type of LCA-Related Advanced Visualization Structures. Research Note RN-KLO-03-03, Department of Precision Engineering, CAD/CAM Research, University of Tokyo, Japan

Otto HE, Mueller KG, Kimura F (2003a): Efficient Information Visualization in LCA: Introduction and Overview. Int J LCA 8 (4) 183–189

Otto HE, Mueller KG, Kimura F (2003b): Efficient Information Visualization in LCA: Approach and Examples. Int J LCA 8 (5) 259–265

Parker A, Cristou C, Cumming B, Johnson E, Hawken M, Zisserman A (1992): The analysis of 3D shape: Psychological principles and neural mechanisms. In: G Humphreys (ed.), Understanding vision. Blackwell, Oxford, UK

Post F J, van Walsum T, Post F H and Silver D (1995): Iconic techniques for feature visualization. in: Proc. of the IEEE Symposium on Information Visualization'95, October 30–31, Atlanta, Georgia, 288–295

Ribarsky W, Ayers E, Eble J, Mukherja S (1994): Glyphmaker: Creating customized visualizations of complex data. IEEE Computer 27 (7) 57–64

Yang-Peláez J, Flowers WC (2000): Information Content Measures of Visual Displays. In: Proc. of the IEEE Symposium on Information Visualization'00, October 9–10, Salt Lake City, Utah, USA, 99–104

Ware C (2000): Information Visualization: Perception for Design. Morgan Kaufman, New York, USA

Watkins DS (1991): Fundamentals of Matrix Computations. Wiley and Sons, New York, USA

Wirth N (1986): Algorithms + Data Structures = Programs. Prentice-Hall, Englewood Cliffs, New Jersey, USA

Received: October 17th, 2003
Accepted: October 28th, 2003
OnlineFirst: October 29th, 2003

About Prof. Dr. Fumihiko Kimura: Dr. Fumihiko Kimura is a professor in the Department of Precision Engineering at the University of Tokyo. He was a research associate at the Electrotechnical Laboratory of the Ministry of International Trade and Industry from 1974 to 1979. He then moved to the University of Tokyo, and was an associate professor from 1979 to 1987.

He created his first solid modeling system GEOMAP in his doctoral work in 1974, and he is one of the pioneers in the field of solid modeling research. Since then he has been active in the fields of solid modeling, free-form surface modeling and product modeling. Today his primary research area is Digital Engineering. His research interests now include the basic theory of CAD/CAM, concurrent engineering, engineering simulation, virtual manufacturing, total product life cycle engineering, environmentally conscious manufacturing and preventive maintenance. He is involved in the product model data exchange standardization activities of ISO/TC184/SC4, and is a national representative of IFIP TC5, a member of IFIP WG5.2 and 5.3, and an active member of CIRP. He is a chairman of the evaluation committee of the IMS Program under METI, the technical committee of the Inverse Manufacturing Forum, MSTC, and other governmental and public committees.

He graduated from the Department of Aeronautics, University of Tokyo, in 1968, and received a Dr. Eng. Sci. degree in aeronautics from the University of Tokyo in 1974.

Appendix

1 Basic manipulation of geometric objects

Homogeneous coordinate representation is useful in describing the manipulation of geometric objects. Problems in $(n+1)$-space corresponding to problems in n-space may have solutions obtained more easily in the $(n+1)$-space than in the lower dimensional space of the original problem (Maxwell, 1951). The homogeneous representation of $x \in \mathbf{R}^3$ with $[x,y,z]$ is $[wx,wy,wz]$ for any $w \neq 0$. Thus an homogeneous point represented by the vector $[x_n,y_n,z_n,d]$ has a corresponding three-dimensional image computed as $[x_n/d,y_n/d,z_n/d]$. Note that in the literature it is customary to use the symbols wx, wy, etc. as diphthongs representing one single value. This should not be confused with the product of x and w.

Geometric transformations are important in generating images of three-dimensional scenes with individual objects in a particular relationship to each other regarding viewpoint, size, location, etc. In the following a basic transformation is represented as a single mathematical entity in the form of a transformation matrix. Complex transformations can be expressed as a sequence of basic transformations which are concatenated by matrix multiplication to yield a single transformation (matrix). Note that the order of the sequence is important since matrix multiplication is not commutative.

The *scaling matrix* denoted as S_{xyz} describes the scaling of the dimensions of a three-dimensional entity in each coordinate direction x, y and z as $[x',y',z',1] = [x,y,z,1]\ S_{xyz}$ and is shown in Eq.8.

$$S_{xyz} = [s_{ij}] = \begin{bmatrix} s_x & 0 & 0 & 0 \\ 0 & s_y & 0 & 0 \\ 0 & 0 & s_z & 0 \\ 0 & 0 & 0 & 1 \end{bmatrix} \tag{8}$$

where sx, sy and sz are the scaling factors.

The *translation matrix* denoted as T_{xyz} describes the translation of a point (x,y,z) to a new point (x',y',z') as $[x',y',z',1] = [x,y,z,1]\ T_{xyz}$ and is shown in Eq.9.

$$T_{xyz} = [t_{ij}] = \begin{bmatrix} 1 & 0 & 0 & 0 \\ 0 & 1 & 0 & 0 \\ 0 & 0 & 1 & 0 \\ t_x & t_y & t_z & 1 \end{bmatrix} \tag{9}$$

where t_x, t_y and t_z are the components of the translation in the x, y, and z directions, respectively.

The *rotation matrices* denoted as R_x, R_y and R_z shown in Eq.10, Eq.11, and Eq.12 describe the rotation about a coordinate axis (see Fig. 8) with a rotation angle θ as $[x',y',z',1] = [x,y,z,1]\ R_n$ with $R_n \in \{R_x,R_y,R_z\}$. The rotation angle is measured clockwise about the origin as regarded from a point on the respective axis.

$$R_x = [r_{ij}] = \begin{bmatrix} 1 & 0 & 0 & 0 \\ 0 & cos\theta & -sin\theta & 0 \\ 0 & sin\theta & cos\theta & 0 \\ 0 & 0 & 0 & 1 \end{bmatrix} \tag{10}$$

$$R_y = [r_{ij}] = \begin{bmatrix} cos\theta & 0 & sin\theta & 0 \\ 0 & 1 & 0 & 0 \\ -sin\theta & 0 & cos\theta & 0 \\ 0 & 0 & 0 & 1 \end{bmatrix} \tag{11}$$

$$R_z = [r_{ij}] = \begin{bmatrix} cos\theta & -sin\theta & 0 & 0 \\ sin\theta & cos\theta & 0 & 0 \\ 0 & 0 & 1 & 0 \\ 0 & 0 & 0 & 1 \end{bmatrix} \tag{12}$$

A closer look at these equations reveals that all three rotation transformations are actually only variants of one and the same schema with a basic rotation matrix permuting the (rotation) axes in a cyclic manner (**Fig. 8**).

Further details of these formulae and additional information on this subject can be found in (Berg et al. 1997, Golub and Loan 1996, Hosaka 1992, Watkins 1991).

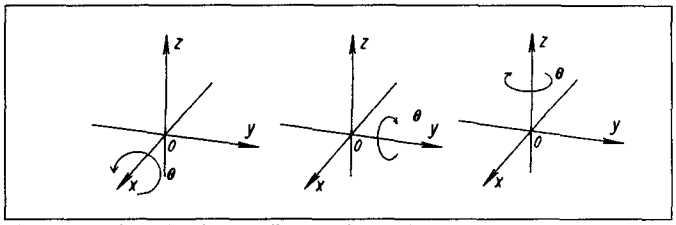

Fig. 8: The three basic coordinate axis rotations

2 Tree data structures

Tree structures are one type of data structure consisting of a set of primitive data elements and other data structures, including also a set of structural relationships among the elements. The representation of such abstracted trees can range from nested sets and nested parenthesis terms to hierarchical graphs as shown in **Fig. 9** and **Fig. 10**.

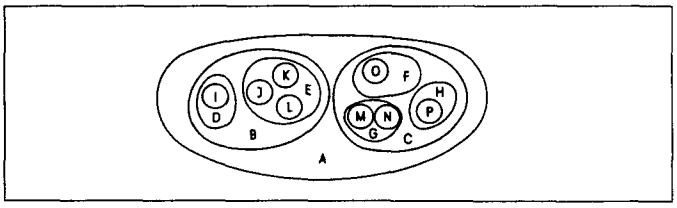

Fig. 9: Tree structure represented as nested sets

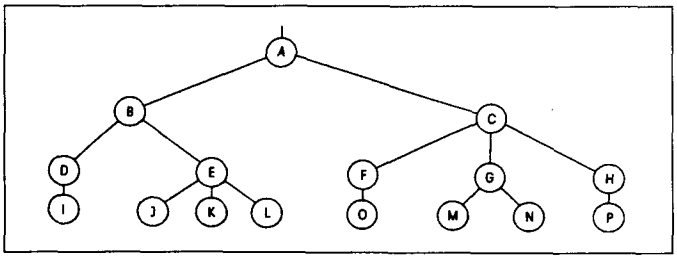

Fig. 10: Tree structure represented as a hierarchical graph

An instance of a tree denoted as t of type T can be recursively defined as a collection of elements which are called nodes with the following structural relationship:

(i) One element denoted as r represents the root of t.
(ii) Other nodes n_i can be partitioned into $k \geq 0$ sub-trees $t_1, t_2, ..., t_k$ such that the root r_m of t_m is a child of r.

The number and type of functions commonly associated with data structures vary with type and structure, though basic operators such as *constructors*, *destructors* and *selectors* to create and delete instances, and access data, are always required. Of further interest in tree structures are functions that determine structural properties in a certain instance. For example, sometimes of interest is the number of nodes of a tree, the number of levels of a tree and the inner path length, which represents the sum of all paths among all nodes. Further details and additional information on this subject can be found in (Aho et al. 1983, Wirth 1986).

3 The product tree

In the following the lists of identified components and parts of the industrial product, subject of analysis, are shown in **Fig. 11** and **Fig. 12**. Components and parts together with their relationships are depicted within the complete product tree as shown in **Fig. 13**.

ID	Component / Part
1	computer & monitor
2	computer
3	color monitor
4	HDD
5	FDD
6	FAX
7	WinFastForce
8	memory
9	keyboard
10	mouse
11	motherboard
12	electric power supply
13	CD-RW
14	IC per piece
15	IC per mass
16	PWB glass epoxy
17	connector
18	capacitor LCR
19	diode
20	transistor
21	resistor LCR
22	electrolytic capacitor per piece
23	cable
24	IC per piece
25	connector
26	capacitor LCR
27	transistor
28	resistor LCR
29	electrolytic capacitor per piece
30	LED
31	PWB paper phenol
32	coil per piece
33	switch
34	IC per piece
35	IC per mass
36	PWB glass epoxy
37	connector
38	capacitor LCR
39	diode
40	transistor
41	resistor LCR
42	electrolytic capacitor per piece
43	coil per piece
44	coil per mass
45	transport per piece
46	transport per mass
47	electrolytic capacitor per mass
48	IC per piece
49	IC per mass
50	connector
51	capacitor LCR
52	diode
53	transistor
54	resistor LCR
55	coil per piece
56	coil per mass
57	IC per piece
58	IC per mass
59	PWB glass epoxy
60	capacitor LCR
61	resistor LCR
62	IC per piece
63	PWB glass epoxy
64	connector
65	capacitor LCR
66	diode
67	transistor
68	resistor LCR
69	electrolytic capacitor per piece
70	cable

Fig. 11: List of components and parts (section 1)

ID	Component / Part
71	LED
72	PWB paper phenol
73	IC per piece
74	capacitor LCR
75	resistor LCR
76	cable
77	LED
78	PWB paper phenol
79	switch
80	IC per piece
81	IC per mass
82	PWB glass epoxy
83	connector
84	capacitor LCR
85	diode
86	transistor
87	resistor LCR
88	electrolytic capacitor per piece
89	coil per piece
90	coil per mass
91	electrolytic capacitor per mass
92	lithium battery
93	packing material
94	IC per piece
95	IC per mass
96	connector
97	capacitor LCR
98	diode
99	transistor
100	resistor LCR
101	electrolytic capacitor per piece
102	cable
103	coil per piece
104	switch
105	coil per mass
106	transport per piece
107	transport per mass
108	electrolytic capacitor per mass
109	chassis
110	IC per piece
111	IC per mass
112	connector
113	capacitor LCR
114	diode
115	transistor
116	resistor LCR
117	electrolytic capacitor per piece
118	cable
119	LED
120	PWB paper phenol
121	coil per piece
122	switch
123	coil per mass
124	electrolytic capacitor per mass
125	CDs
126	FDs
127	manual
128	cable (power)
129	CRT assembly
130	PCB assembly
131	cabinet
132	packaging box
133	packaging material
134	shield
135	others

Fig. 12: List of components and parts (section 2)

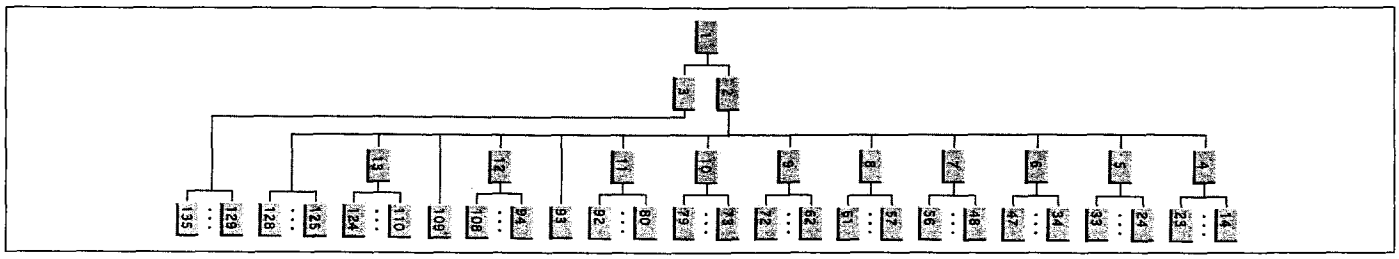

Fig. 13: The product tree